Magnetic "blocking" in very dilute (Eu_xSr_{1-x}) S: Experiment versus theory

G. Eiselt and J. Kötzler
Institut für Festkörperphysik, Fachgebiet Technische Physik Technische Hochschule Darmstadt, 6100 Darmstadt, West Germany

H. Maletta
Institut für Festkörperforschung, Kernforschungsanlage Jülich, Postfach 1913, 5170 Jülich 1, West Germany

D. Stauffer
Institut für Theoretische Physik, Universität zu Köln, Zülpicher Str. 77, 5000 Köln 41, West Germany

K. Binder
Institut für Festkörperforschung, Kernforschungsanlage Jülich, Postfach 1913, 5170 Jülich 1, West Germany
(Received 3 October 1978; revised manuscript received 23 October 1978)

Both ac and dc magnetic susceptibilities have been measured for Eu concentrations $x = 0.025$, 0.05, and 0.10 over temperatures in the range from 0.007 K to 4 K. While the dc susceptibility is found to exhibit no peak down to 7 mK, the ac susceptibility shows two distinct maxima around 15 mK and 200 mK. The frequency dependence of the two-peak positions $T_a(\nu)$ and $T_b(\nu)$ can be adequately described by an Arrhenius law in the range of our measurements from $10-10^6$ Hz. The results for the peak at the higher-temperature T_b are explained quantitatively for $x = 0.025$ and $x = 0.05$, without adjustable parameters, by a model of small random Eu clusters. They consist of Eu atoms coupled by strong exchange forces between nearest-and next-nearest neighbors, and experience energy barriers mainly due to the intracluster dipolar energy. One particular configuration, two nearest-neighbor Eu atoms bonded ferromagnetically, produces the anomaly near T_b. Thus $T_b(\nu)$ arises from ordinary superparamagnetic behavior. In spite of the very low temperatures investigated, quantum-mechanical cluster reorientation is shown to be negligible due to the high-spin quantum number of Eu, even for the smallest clusters. The newly found maximum at the lower-temperature T_a is interpreted as a result of intercluster dipolar energy, giving good agreement for the order of magnitude of T_a and its concentration dependence. Its dependence on frequency remains to be explained.

I. INTRODUCTION

The low-temperature behavior of disordered magnets has recently been the subject of much theoretical and experimental research. Of particular interest are alloys like 1 at.% Fe in Au where the long-range oscillatory RKKY interaction via the conduction electrons are responsible for a new type of magnetic order, the so called spin-glass phase.[1] There is no consensus on the interpretation of the spin-glass phenomena. Often[2–4] the concept of "superparamagnetic clouds" is applied, so that around the spin-glass temperature T_f nothing else but the blocking of superparamagnetic clouds occurs. Binder[1] already has objected to these attempts of explanation because, as an important distinction, the interaction between the clouds has to be taken into account in real spin-glass materials, too. Recently, Maletta and Felsch[5] have obtained experimental evidence on the spin-glass-like properties also in the insulating system $(Eu_xSr_{1-x})S$ with concentrations $x \leq 0.5$, caused by the competition of ferro- and antiferromagnetic exchange interactions of predominant short range. Hence, competing interactions independent on the range appear to be necessary for spin-glass behavior. The same authors[5] have observed the low-concentration limit of the spin-glass regime in $(Eu_xSr_{1-x})S$ at the percolation threshold $x_p = 0.13$.

In the very dilute concentration regime of insulating (EuSr)S dipole-dipole coupling must play a dominant role at very low temperatures. Holtzberg *et al.*[3] have already measured the remanent magnetization and its relaxation effects in such samples, and claimed to have herewith an example of a dipolar spin glass. Such effects, however, are also well-known features of superparamagnetism. In a recent paper by Tholence *et al.*,[6] new measurements of the temperature and frequency dependence of the susceptibility are interpreted quantitatively by a blocking of pairs of nearest-neighbor Eu ions.

In the present paper a detailed experimental and theoretical study on the magnetic properties of $(Eu_xSr_{1-x})S$ below x_p is reported. Measurements of the ac susceptibility, in dependence on frequency and concentration x, yield two maxima at temperatures T_a and T_b, whereas the static susceptibility remains increasing with decreasing T down to the lowest accessible temperature of 7 mK. The susceptibility near T_b can be described by a model of superparamagnetic clusters. Their structure is defined by the exchange interactions, while their dynamics is mainly determined by energy barriers due to the intracluster dipolar energy. The Appendix of the present paper gives detailed cluster properties and determines which of the many cluster configurations is responsible for the susceptibility maximum at T_b. We agree with the conclusion of Ref. 6 concerning the blocking of pairs and show explicitly that more complicated clusters are less important for T_b. The second susceptibility maximum at the lower-temperature T_a, which has not been observed in[6], is shown to be predominantly caused by long-range dipolar interactions between the clusters. If one likes to introduce the concept of a dipolar spin glass[3], our present understanding suggests to call T_a, not T_b, a spin-glass temperature. The paper is organized as follows: After the description of the experimental apparatus given in Sec. II, the results of the measured susceptibilities in very dilute (EuSr)S are reported in Sec. III. Both dc and ac susceptibility measurements have been performed, the ac method with varying measuring frequency. In the following two sections, the theoretical model is outlined and its numerical results are compared with the measured curves. First (Sec. IV) free clusters are considered, while as a next step (in Sec. V) the weak interactions between the clusters are approximately taken into account in the calculations.

II. EXPERIMENTAL TECHNIQUES

The low temperatures were generated by means of a ^{3}He-^{4}He dilution refrigerator delivering a cooling power of 50 μW at 100 mK (Ref. 7). Careful protection of the cryostat against rf stray fields and mechanical vibrations allowed minimum temperatures of 11 and 7.2 mK to be reached in the continuous and single cycle modes, respectively. In order to minimize heating from the rf fields applied during the measurements of the ac susceptibility, the mixing chamber was fabricated using epoxy resin (see Fig. 1). The temperatures were measured by a miniature carbon resistor (Matsushita 56 Ω $\frac{1}{8}$ W) attached to the sample holder. Copper foils soldered to the electrical leads within the mixing chamber improved the thermal contact of the carbon thermometer to the cooling medium. We calibrated the temperatures

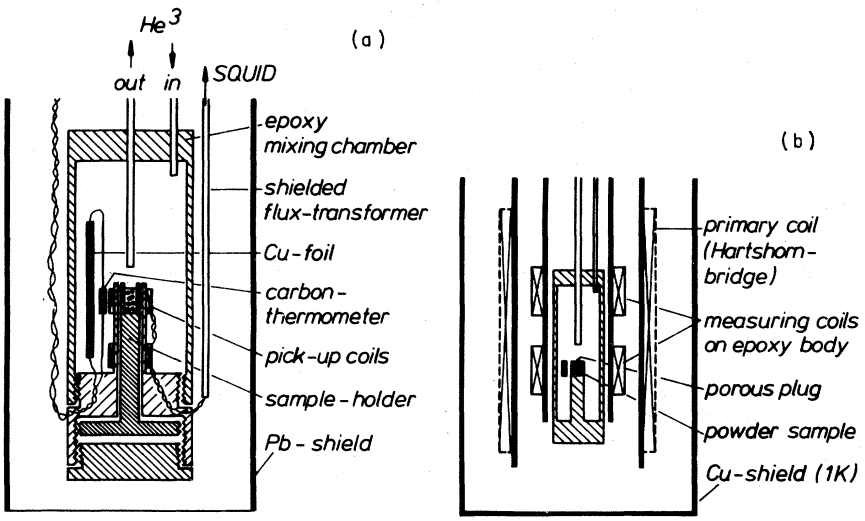

FIG. 1. Low-temperature assembly for measuring (a) dc susceptibility, and (b) ac susceptibilities between 12 Hz and 1 MHz. The insert is under high vacuum and shielded from the ^{4}He bath by a 1 K Cu shield.

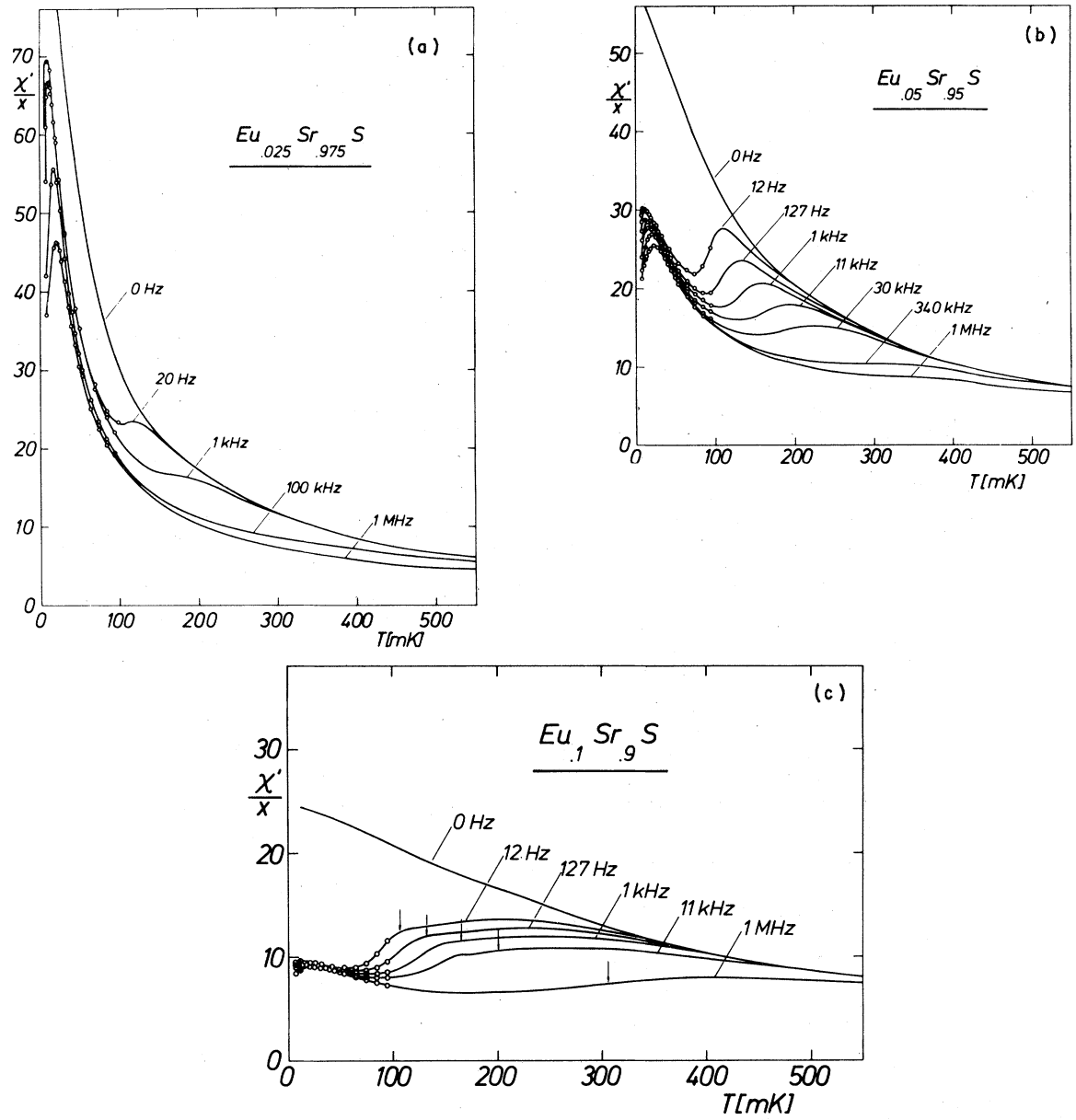

FIG. 2. Temperature dependence of the static susceptibility and of the real part of the dynamic susceptibilities of $Eu_xSr_{1-x}S$ for $x=0.025$ (a), $x=0.05$ (b), $x=0.10$ (c). Note that all curves are normalized to x. The ac data were taken continuously above 100 mK. Below 100 mK circles indicate pulse-type measurements, through which full lines have been drawn as guides to the eye. Full circles show data associated with extraordinary long measuring times (12 h).

between 1 and 4 K against a Ge thermometer, and below 1 K by measuring the susceptibility of a standard CMN sample. In order to eliminate uncertainties in thermometry after changes in the low-temperature measuring arrangement (see Fig. 1) we repeated the calibration each time in situ by replacing the measuring sample with CMN.

The dc susceptibility was determined from measurements of the magnetization by a superconducting quantum interference device (SQUID). Figure 1(a) shows the essential parts of the apparatus: the flux of the sample being magnetized by the trapped magnetic (earth) field of 0.40 G, is picked up from a pair of astatic coils and fed via a superconducting flux transformer to the SQUID of the pointcontact type. The electronics[8] coupled to the SQUID delivers a voltage proportional to the flux. This signal is converted into units of susceptibility (per unit volume) by ad-

justing it to the susceptibility of the sample, measured independently between 1 and 4 K in a calibrated mutual inductance bridge (precision: 3%). Magnetization data were continuously recorded during the cooling process of 24 h from 4.2 K to 11 mK. Thereafter the ^{3}He supply to the mixing chamber was shut off, reaching the absolute minimum temperature in another hour. Thermal equilibrium between sample and thermometer was checked by fixing several temperatures by means of heater during the warming-up period. Within the long-term stability of the SQUID of better than 1% of the effect, no thermal hysteresis could be detected.

The dynamic susceptibilities were measured by means of two different ac bridges applying lock-in detection. Between 12 Hz and 1 kHz a Hartshorn bridge[9] was employed while at higher frequencies, 11 kHz $\leq \nu \leq$ 1 MHz, a four-inductance bridge of the Wheatstone type[10] was used. In order to obtain a sufficiently large filling factor of the measuring coil, in both cases the coil systems were put around the mixing chamber within the low-temperature vacuum jacket [see Fig. 1(b)]. Down to 100 mK the ac susceptibilities could be recorded continuously as a function of temperature. At lower temperatures rf heating of the resistance thermometer was observed, so that measurements were carried out by applying short rf pulse at discrete temperatures (cp Fig. 2). Changing the ac amplitude by a factor of 3 about the measuring value of approximately 0.5 G, we found no effect on the ac susceptibility of the (Eu_xSr_{1-x})S samples, so that we assume having measured their linear response. The (Eu_xSr_{1-x})S samples under study were prepared from powder material weighting 50 mg for the SQUID and about 250 mg for the ac measurements. They were immersed directly into the cooling liquid in order to ensure a good thermal contact.

III. MEASURED SUSCEPTIBILITIES

The principal experimental results are shown in Figs. 2(a)–(c), i.e., the dc and ac susceptibilities for three different Eu concentrations versus temperatures below 550 mK. All susceptibilities are normalized to the nominal Eu content and for reasons of better intercomparison they were reproduced on the same scale.

Considering first the static limit we observe a significant enhancement of the susceptibility with decreasing concentration. It may be plausible to ascribe this effect at a first glance to the larger number of free single spins. We find for all x, that the increase of the dc χ with decreasing T starts to weaken, at the lowest temperatures even for the 2.5% sample without, however, reaching a maximum in the range of accessible temperatures ($T \geq 7.2$ mK). We should mention that after having established thermal equilibrium between bath and thermometer at no temperature changes of the magnetization with time were detected.

Differences between the dc susceptibilities are observed, too, at higher temperatures (see Fig. 3). While for the lowest concentration an almost ideal Curie law $\chi/x = \lambda/(T-\theta)$ is observed over more than one decade in temperature (3–0.3 K), yielding for the Curie constant $\lambda = 3.01(2)$ K, i.e., the value of the concentrated EuS and $\theta = 0.05(2)$ K, a more complicated behavior occurs at larger concentrations: coming from low temperatures their susceptibilities for both $x = 0.10$ and 0.05 intersect that of the $x = 0.025$ sample around 0.3 K and become then increasingly larger.

The most interesting phenomenon in the ac susceptibilities is the occurrence of a double maximum structure, labelled T_a and T_b, in each of the three samples. Only the maximum T_b at the higher temperature was observed by Tholence *et al.*[6] and only for a smaller frequency range. It is obvious from Figs. 2(a)–(c), that the relative height of the two maxima changes drastically with concentration: whereas in the $x = 0.025$ sample the low-temperature peak dominates clearly, its importance diminishes in

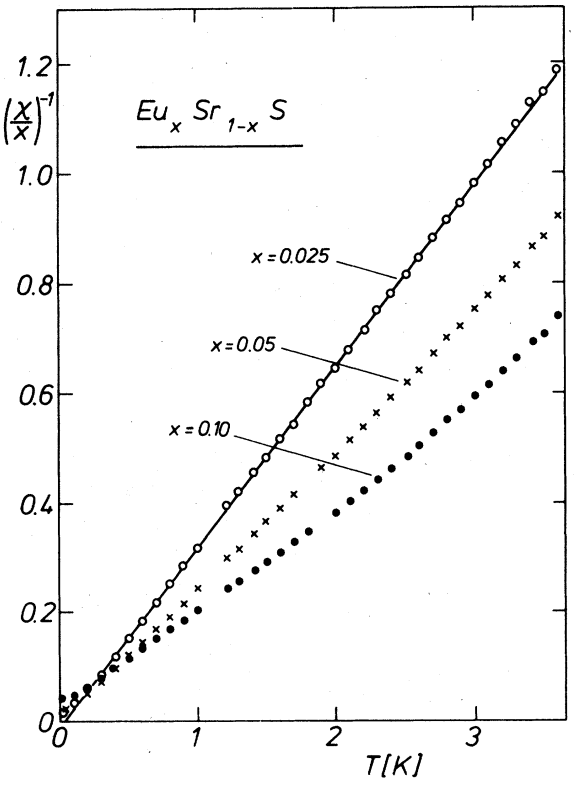

FIG. 3. Inverse of the static susceptibility of $Eu_xSr_{1-x}S$ at higher temperatures normalized to x.

the more concentrated samples. A quantitative comparison of these amplitudes with our theory is given in Sec. V (Table II).

The frequency dependencies of the two maxima are depicted in Fig. 4 employing the conventional plot T^{-1} versus log ν. Note that the accuracy by which T_a and T_b can be determined from the measuring curves is much higher as it might appear from Fig. 2. The relatively larger errors of T_a are mainly related to difficulties with the thermometry around 10 mK. All data in Fig. 4 appear to be consistent with Arrhenius' law in whole range of frequencies

$$R = R_0 \cdot e^{-E_a/k_B T},$$

according to which the temperatures of the ac susceptibility maxima are expected to decrease linearly with log ν. The energy barriers E_a and the amplitudes R_0 obtained from weighted least-square fits (see full lines in Fig. 4) are listed in Table I.

Representing our results for T_b in Fig. 4(a) we have also included the recently published data.[6] Though there exists a small temperature shift between both data sets resulting in slightly different values for E_a and R_0 (see Table I), the general feature of our findings is similar: T_b proves to be independent on concentration up to $x = 0.05$, while in Ref. 6 this was supposed to be the case up to $x = 0.03$ only. It is perhaps interesting to note that the ac susceptibilities of the $x = 0.10$ sample still shows a spurious indication of this concentration independent T_b peak, being indicated by arrows on the low-temperature flank of the broad maximum around 250 mK in Fig. 2(c). — The dashed line in Fig. 4(a) represents the result of our calculations for T_b outlined in Sec. V. We believe that the agreement is quite remarkable with regard to the fact that no adjustable parameter enters into the theory.

On the other hand we have so far no quantitative description of the results for the low-temperature maximum at T_a, the frequency dependence of which

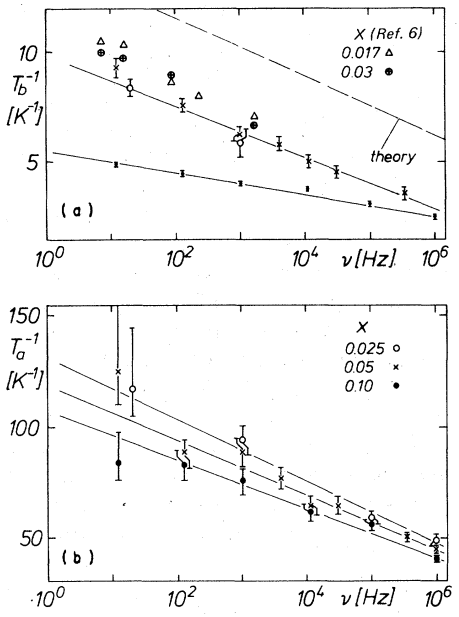

FIG. 4. Temperatures of the maxima in the ac susceptibility as a function of frequency. Full lines represent Arrhenius laws adjusted to our data with parameters given in Table I. (a) Upper maximum T_b. Dashed line represents the theoretical result (Sec. V) for the limit of low concentrations x. (b) Lower maximum T_a.

suggested an analysis in term of an Arrhenius law, too. We find a systematic increase of the energy barrier E_a and of the prefactor R_0 with growing Eu concentration x (see Table I). If we assume that the maximum at T_a arises from dipolar interactions between different clusters as in our model (Sec. V), than these forces and the resulting energy barriers should indeed increase with x. Perhaps the observed increase of the coefficient R_0 with concentration suggests an influence of increasing cluster size s_k [cf. Eq. (4b)].

TABLE I. Energy barriers and amplitudes of Arrhenius' law applied in the analysis of T_a and T_b. For T_b we have included the results of the Grenoble group and of our theory. Uncertainty of values for R_0 is one order of magnitude.

		T_b		T_a	
	x	$\frac{E_a}{k_B}$ (K)	$R_0(10^9\ \text{sec}^{-1})$	$\frac{E_a}{k_B}$ (K)	$R_0(10^9\ \text{sec}^{-1})$
Theory	≤0.05	1.7	25	...	...
Ref. 6	≤0.03	1.7	0.17	...	...
this work	0.025			0.17(2)	3
		2.0(1)	0.3		
	0.05			0.19(1)	4
	0.1	4.7(3)	90	0.21(2)	5

IV. THEORETICAL MODEL: FREE CLUSTERS

The basic idea behind the theoretical model is that we restrict ourselves to such low concentrations of magnetic atoms ($x \leq 0.05$) that complicated collective phenomena like the percolating phase transition (at $x \simeq 0.13$) play no role in our model. At these low concentrations most of the atoms will be concentrated in very small clusters (triplet, pairs, and isolated spins) which can be treated exactly in their static and dynamic properties. Thus no free parameters enter this model, and we will see that it predicts at the correct temperature a drastic deviation from the Curie law. (The principles of this theoretical model have some similarity with an earlier dynamical percolation model[11]; but now we are interested in real experiments, not in critical phenomena at astronomically large times[11]). More sophisticated methods are employed later to improve the agreement with experiment.

Following Passell *et al.*,[12] we take the magnetic Eu atoms as spin-$\frac{7}{2}$ moments localized on an fcc lattice, with nearest and next-nearest interactions only. The nearest-neighbor coupling is ferromagnetic, the next-nearest-neighbor coupling is antiferromagnetic, with a ratio of -0.5 between antiferro- and ferromagnetic coupling constants. (Their absolute value does not enter our results). Since the critical temperature of EuS is about 16.5 K and we restrict ourselves to temperatures below 1 K we assume that the thermal energy is not sufficient to break the exchange interaction. The Eu atoms are assumed to be distributed randomly among the lattice sites, with no change in the interaction constants compared with pure EuS. Any group of magnetic atoms connected by nearest- or next-nearest-neighbor interactions is called a "cluster", as is known from percolation theory.[13] According to our assumptions thermal fluctuations cannot break the bonds within one cluster; thus only the spin orientation of the cluster as a whole can change in time. In general each cluster has only two equivalent directions into which its magnetization direction can show, and these two directions are antiparallel to each other. Thus the superparamagnetic cluster behaves like a spin in a $S = \frac{1}{2}$ Ising model.

With these assumptions the equilibrium magnetic behavior can be calculated with the methods known from percolation theory[13] as applied to dilute magnets. The average number n_k of clusters of configuration k, with s_k spins in each of these clusters, is[14]

$$n_k(x) = g_k x^{s_k}(1-x)^{t_k} . \tag{1}$$

Here t_k is the perimeter of configuration k, i.e., the number of nonmagnetic atoms which are nearest or next-nearest neighbors of the magnetic Eu atoms in the cluster. The multiplicity g_k counts the number of different orientations which a cluster of given size and shape can have due to rotations in the lattice; also mirror images contribute to g_k. Figure 5 shows the cluster configurations for $s = 1, 2,$ and 3; in the Appendix their multiplicities and other properties are listed. By evaluating Eq. (1) for these and larger clusters, Dalton *et al.*[15] estimated the percolation threshold in this problem to be at about $x_c = 0.136$; for larger concentrations x also one infinite cluster will appear. Our concentrations later will always be appreciably smaller than this percolation threshold x_c.

For each configuration k the spins are parallel or antiparallel to each other such that the total exchange energy is minimized; in our evaluation of this minimum energy configuration we neglect the weaker dipolar forces taken into account later for the energy barriers. In some cases a "loose" spin can occur, i.e., one spin experiences conflicting forces from its neighbors which exactly cancel each other; then this loose spin behaves like an isolated magnetic atom. However, no loose spins were possible for small clusters ($s_k \leq 4$); and for larger clusters up to $s_k = 10$, less than 1% of the spins were loose. Thus we neglect the loose spins, i.e., we treat them as rigidly coupled to the cluster they belong to. The magnetization m_k in each cluster is determined by the difference between the number of up spins and the number of down spins in the minimum-energy distribution of spin orientations; in units of the magnetic moment μ per spin the magnetization varies between zero and s_k and is also listed in the Appendix. The dipolar forces within a cluster produce an easy axis; ϕ is the angle which this axis has with the direction of the magnetic field H. Thus in thermal equilibrium the average magnetic moment μ_k in the field direc-

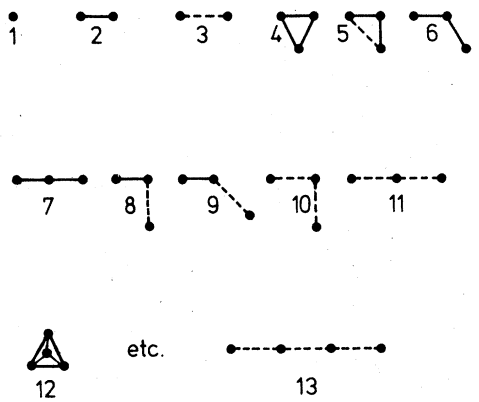

FIG. 5. List of small clusters formed by Eu atoms in an fcc lattice. The solid lines are ferromagnetic nearest-neighbor bonds, the dashed lines antiferromagnetic next-nearest-neighbor bonds. For $s = 4$ clusters, only the smallest and the largest are shown. The numbers below each cluster give its index k, as listed in the Appendix.

tion is for cluster configuration k,

$$\mu_k = \mu m_k \cos(\phi) \tanh(\mu m_k H \cos\phi / k_B T) \ . \quad (2)$$

Therefore the average contribution, of all clusters with configuration k, to the susceptibility is $\frac{1}{3}\mu^2 m_k^2 n_k(x)/k_B T$ where the average over $\cos^2\phi$ has been replaced by $\frac{1}{3}$. Summing up over all possible cluster configurations we get for the total static susceptibility in thermal equilibrium

$$\chi(t \to \infty) \propto \sum_k m_k^2 g_k x^{s_k}(1-x)^{t_k}/T \ , \quad (3)$$

as is well known basically from the theory of superparamagnetism. This formula is also valid for isolated spins.

To discuss the time-dependent properties of our model we assume that each configuration k flips its spin orientation with a rate R_k varying according to an Arrhenius law, i.e., proportional to $\exp(-E_k/k_B T)$ where E_k is the energy barrier for this flipping process of the whole cluster. In spite of the fact that we consider temperatures as low as 10^{-2} K flips by quantum tunneling processes are negligible in comparison to the thermal reorientation, due to the large spin quantum number of the clusters, which nearly correspond to "classical" spins. Note that for ferromagnetic triplets we would have to consider transitions from

$|\lambda\rangle = |SS\rangle$ with $S = 3S_{Eu} = \frac{21}{2}$ to $|\mu\rangle = |S\ -S\rangle$,

which are produced by that part $\mathcal{H}'$ of the dipolar interaction Hamiltonian[3]

$$\mathcal{H}_{dip} = \sum_{i<j=1,2,3} \left[(\vec{\sigma}_i \vec{\sigma}_j) r_{ij}^{-3} - \frac{3(\vec{\sigma}_i \vec{r}_{ij})(\vec{\sigma}_j \vec{r}_{ij})}{r_{ij}^5} \right],$$

which does not commute with the operator $\vec{S}$ (which is proportional to the operator of the magnetization $\vec{\sigma}_1 + \vec{\sigma}_2 + \vec{\sigma}_3$). Because of the relations[16]

$$S_\pm |SM\rangle = [(S \mp M)(S \pm M + 1)]^{1/2} |SM \pm 1\rangle$$

the transition frequency ω {which would be $\omega = (2\pi/\hbar)|\langle\lambda|\mathcal{H}'|\mu\rangle|^2$ in first-order perturbation theory} is zero in the first $2S-1$ orders of perturbation theory. The order of magnitude of the first nonzero order is estimated as $\omega \propto [(\sigma^2/a^3\tilde{J})^{2S-1}(\sigma^2/a^3)]^2$, where σ is the magnetic moment of Eu ions, a the nearest-neighbor distance, $\tilde{J} = S(S+1)J$, and J is the nearest-neighbor exchange constant.[17] I.e., $\sigma^2/a^3\tilde{J}$ measures the ratio between the nearest-neighbor dipolar energy to exchange energy: since this small quantity is raised to such a high power these tunneling flips are completely negligible as compared to thermal ones (note that this conclusion would be different for $S = \frac{1}{2}$ ions). The energy barrier E_k in the classical estimate is calculated from $\mathcal{H}_{dip}$ by treating the $\vec{\sigma}_i$ as classical vectors $\vec{\mu}_i$. Since the strong exchange forces between the spins make all vectors $\vec{\sigma}_i$ either parallel or antiparallel to each other, the dipolar energy E_{dip} depends on only two angles θ_1, θ_2 characterizing the direction of the cluster magnetization. The two equilibrium orientations are given by the absolute minimum in the energy surface $E_{dip}(\theta_1, \theta_2)$. For each configuration we have to search for a saddle point in this energy surface which is determined as the highest point in the lowest-energy path connecting the two minima of the dipolar energy. The difference between E_{dip} at the saddle point and E_{dip} at the minimum is then the energy barrier E_k which is hindering the free rotation of the cluster magnetization.

If a field H is suddenly switched on at time $t=0$, then the cluster orientations lag behind their equilibrium orientations by a factor $1-\exp(-R_k t)$, where R_k is the rate with which clusters of configuration k are flipping. We take

$$R_k = R_0 \exp(-E_k/k_B t) \quad (4a)$$

as is generally assumed for thermal processes where an energy barrier E_k has to be surmounted. In the present case, thermal lattice vibrations (phonons) may induce the spin clusters to jump over the barrier. Therefore, we assume the proportionality factor R_0 in Eq. (4) to vary linearly with T. Moreover a large cluster feels more such phonon attempts to overturn its direction, and thus the proportionality factor should also increase with the size s_k of the cluster. Different phonons will act randomly and independently, and thus a prefactor varying as $s_k^{1/2}$ seems the most plausible choice. Taking the microscopic time as 10^{-11} sec at $T=1$ K by assuming the classical formula for the attempt frequency $\omega \approx k_B T/\hbar$, we thus arrive at

$$R_k = s_k^{1/2} T \times 10^{11} \exp(-E_k/k_B T) \ \text{sec}^{-1}\text{K}^{-1} \quad (4b)$$

as our cluster flip rate. However this classical prefactor is an upper limit for the actual attempt frequency and hence is at best an order-of-magnitude estimate, and thus our time-scales are not very accurate. Equation (4b) is assumed to be valid for energy barriers E_k much larger than the thermal energy $k_B T$. Moreover, the present accuracy of our experimental data presumably does not allow a definite conclusion about the effect of the temperature and cluster size on the prefactor for the rate R_k. With these assumptions, the time lag in the motion of clusters due to the energy barriers leads to an effective time-dependent susceptibility per spin $\chi \equiv \partial M/\partial H \simeq M/H$ in the linear response regime with

$$\chi(t) \propto \sum_k m_k^2 n_k(x) \frac{1 - e^{-R_k t}}{Tx} \ . \quad (5)$$

Computer evaluation of Eq. (5) for times between 10^{-11} sec and 10^4 sec gives for fixed time t a roughly monotonic decay of the susceptibility with increasing temperature, except for a maximum near $T = T_b(t)$,

as shown in Fig. 6 for $x = 0.05$. The variation of T_b with time is shown in Fig. 7. The value of T_b found in this theory agrees well with the position of the second maximum in the experimental susceptibility as a function of temperature. We find this agreement remarkable since no free parameters and not even the value of the exchange energy are used to fit our theory to the experiments.

As a function of time the maximum at T_b becomes less and less pronounced the smaller the observation time, i.e., the larger the frequency is. We show this effect in the three inserts of Fig. 6 where the behavior near T_b is shown enlarged, for $t = 10^{-8}$, 10^{-2}, and 10^4 sec. Similarly the anomaly is less pronounced for smaller concentrations as is indicated in the insert of Fig. 7. But these data also show that the position of T_b is quite independent of concentration.

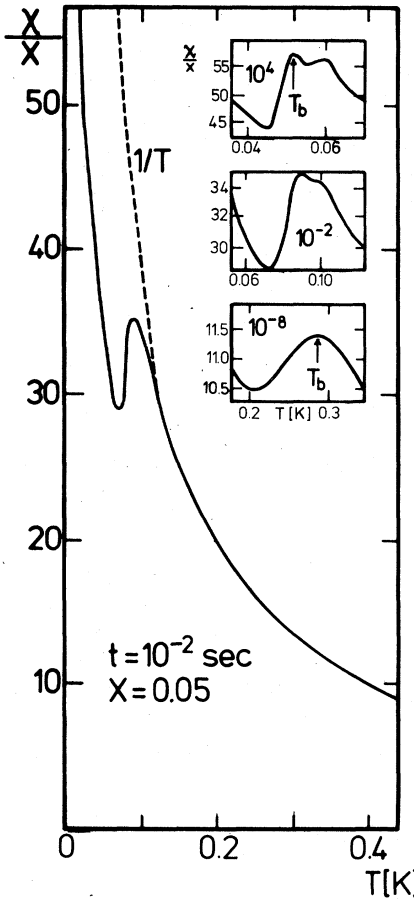

FIG. 6. Plot of susceptibility vs temperature for $t = 10^{-2}$ sec and $x = 0.05$. The dashed line is the equilibrium susceptibility. The three inserts show the anomaly near T_b for $t = 10^4$ sec (top), 10^{-2} sec (middle), and 10^{-8} sec (bottom).

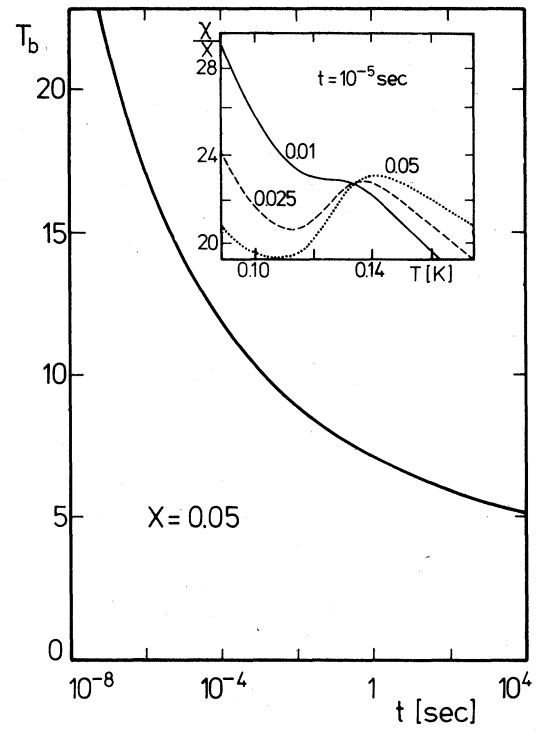

FIG. 7. Variation of the position of the anomaly with time at $x = 0.05$. The insert shows the anomaly for various x, as indicated.

If plotted as a function of time (not shown) the susceptibility curves increase monotonically, roughly linear in log t, and vary somewhat with concentration. [Note that we normalized χ as the susceptibility per spin by dividing in Eq. (5) by the concentration x.] In the linear response regime these data show how the magnetization approaches very slowly its equilibrium value, which it still has not reached after 10^4 sec. (The simplicity of our model would make it easy to calculate the nonlinear response also, for large magnetic fields).

Our model of free clusters, therefore, has given a characteristic temperature T_b varying logarithmically with time but roughly independent of concentration; the numerical value of T_b agrees roughly with our experimental findings and those of Tholence *et al.*[6]; these authors used a similar interpretation as we did but did not give a quantitative study. No free parameters or ambiguous fitting procedures were involved. However, if the attempt frequency at 1 K would be adjusted to 10^9/sec, excellent agreement between theory and experiment were obtained [cf. Fig. 4(a)]. What is missing in this model is the lower maximum in the susceptibility which we observed at T_a experimentally. Thus we now proceed to a more refined model.

V. THEORETICAL MODEL: INTERACTING CLUSTERS

In the simple model described above all magnetic interactions between different clusters were neglected. This approximation is correct as long as only strong exchange interactions (between nearest and next-nearest neighbors) are taken into account. By definition all exchange-coupled spins are grouped into one cluster, and no exchange forces between different clusters exist. However, the dipole-dipole interaction between the spins decreases only as 1/ (distance)^3, and therefore is still coupling different clusters. We had taken into account already the intracluster dipolar forces in calculating the energy barrier E_k for single clusters. Now we need intercluster interactions produced by the same dipolar forces. Since the distances within a cluster are smaller than those between clusters the intercluster forces can be expected to be much smaller than the intracluster forces. But at the very low temperatures near the lower maximum T_a these weak forces may become relevant.

Taking into account these weak forces is an unsolved problem. We have many "particles" (clusters) interacting with forces varying in strength and direction. A gross simplification would be the Edwards-Anderson model of spin glasses[18] where all particles are taken as equal and where only the forces between them vary randomly in direction and strength. Binder[19] has suggested to regard each unit of the Edwards-Anderson model as a cluster. Our present theory gives the needed distribution of magnetic moments for these clusters in the theory of Ref. 19, a distribution approximated there by a delta function. However, even with this simplification it is at present controversial whether or not this model has an equilibrium phase transition (see Ref. 20 with earlier literature). Thus no attempt was made here for a sophisticated theory of dipolar cluster-cluster interactions; instead similar to the simple mean-field approximation of Klein, Brout, and Marshall,[21] we try to give an order-of-magnitude estimate for this cluster-cluster interaction by calculating a distribution of dipolar fields H_d acting on each cluster. We will ignore some correlations between this field and the orientation of the cluster on which it acts.

One given cluster feels the influence of the surrounding clusters as a dipolar field H_d; more precisely H_d is the component of the dipolar field in the direction of the cluster magnetization. Since the distribution of other clusters and their orientation is quite disordered, the dipolar field H_d is not unique but follows a probability distribution $P(H_d)$, with $P(-H_d) = P(H_d)$ for symmetry reasons. When we calculate H_d we neglect, in the spirit of a complicated mean-field approximation, the influence which the orientation of the given cluster has on the orientation of its neighbors. Thus a Monte Carlo computer simulation was devised which distributed for $x = 0.05$ on a lattice randomly the pointlike clusters with random orientation of their magnetic moment. [Concentrations $n_k(x)$ and magnetic moments m_k were taken as derived in Sec. VI]. The resulting field distribution $P(H_d)$ was found to follow a Lorentzian in this Monte Carlo experiment,

$$P(H_d) \propto (\Delta^2 + H_d^2)^{-1} , \tag{6}$$

with a width $\mu\Delta/k_B$ of about 0.009 K at $x = 0.05$. Since dipole forces vary as r^{-3}, i.e., as the concentration, we take the width to be $\mu\Delta/k_B = 0.18x$ K in general.

This field H_d changes the tanh (h) for the magnetization in Eq. (2) into tanh $(h + h_d)$ with the reduced fields

$$h_d = \mu m_k H_d / k_B T, \quad h = \mu m_k \cos(\phi) H / k_B T .$$

Thus the initial susceptibility now carries a correction factor $\cosh^{-2}(h_d)$ instead of unity. Integration over $P(H_d)$ is accomplished by a simple interpolation formula and leads to susceptibilities which are finite for $T \to 0$. This strong deviation from the divergence of the Curie law goes in the desired direction but is not enough to give the pronounced maximum at $T_a \neq 0$.

We think that this Monte Carlo result (6) does not give the correct behavior for $H_d \to 0$ where Eq. (6) predicts a finite probability. Such a result of maximum probability for zero field was also predicted by mean-field approximation of spin glasses but in reality in an Ising spin glass the probability nearly goes to zero if the field goes to zero.[22] Similarly we modify for our dilute magnet the initial result (6) to accomodate $P(H_d = 0) = 0$. Let be $P(H_d \to 0) \propto |H_d|$ for small fields, with the proportionality factor taken as $1/\Delta^2$ in order to give $\int_0^\infty P(H_d)\, dH_d = 1$. This linear increase is about all we need to know on $P(H_d)$.

To evaluate the susceptibility we need the correction factor

$$\int_0^\infty P(H_d) \cosh^{-2}(h_d)\, dH_d$$

which equals $\int_0^\infty P(H_d)\, dH_d = 1$ for high temperatures ($k_B T >> \mu\Delta$), and then gives again our old result (5). In the opposite limit of low temperatures only $P(H_d \to 0)$ is important, giving the correction factor as

$$\int_0^\infty \Delta^{-2} H_d \cosh^{-2}(h_d)\, dH_d = \ln(2) \left(\frac{k_B T}{\Delta m_k \mu} \right)^2 .$$

Interpolation between these two limits gives

$$1/[1 + (\mu m_k \Delta / k_B T)^2 / \ln(2)]$$

as our correction factor for the susceptibility due to dipolar interactions between clusters. Thus in our

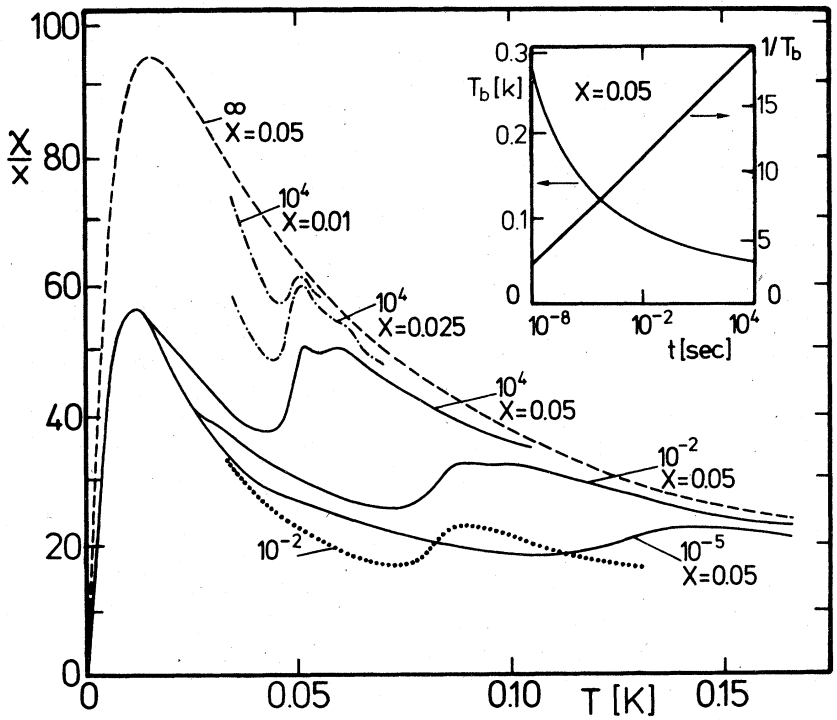

FIG. 8. Results for the improved model: Variation of susceptibility with temperature for $x=0.05$ (solid lines). The numbers give the time in sec; the dashed line is the equilibrium susceptibility. The dashed-dotted lines give results for $x=0.025$ and $x=0.01$ the dotted line gives results for $x=0.05$ when all clusters larger than pairs are ignored. The insert shows the Arrhenius law for the position of the second maximum at T_b.

improved model we have

$$(\chi T) \propto \sum_k m_k^2 n_k(x) \frac{1-e^{-R_k t}}{1+0.05 m_k^2 x^2 T^{-2}} \qquad (7)$$

if the temperature T is expressed in Kelvin. We used

$$(\mu\Delta/k_B)^2/\ln(2) = 0.05\ \mathrm{K}^2 x^2 .$$

This model produces the desired maximum at T_a, Fig. 8, with

$$T_a(x=0.05) \cong 0.011\ \mathrm{K} ,$$

$$T_a(x=0.025) \cong 0.005\ \mathrm{K} ,$$

$$T_a(x=0.001) = 0.002\ \mathrm{K} .$$

Figure 8 also shows that the maximum is independent of time for $10^{-8} \leq t \leq 10^2$ sec. Since the mean strength Δ of the dipole interaction varies as the concentration x, the proportionality of T_a to x is not surprising. And since the influence of the dipolar cluster-cluster interaction comes through a field applied to the cluster, not through an energy barrier hindering its motion, the deviation from the Curie law for small temperatures is an equilibrium effect near T_a, evident even from the static susceptibility for $t=\infty$. The main effect of the cluster-cluster interaction is to give a preferred direction to the many isolated spins which otherwise could rotate freely. [Indeed, replacing m_k^2 by m_k in Eq. (7) does not shift T_a appreciably].

We next discuss possible modifications of our basic model: The exchange interactions between third-nearest neighbors could be important[12]; or the distribution of Eu atoms is not entirely random with Eu atoms showing an enhanced probability to be close to each other ("chemical clustering").

The first effect, interactions with third-nearest neighbors, would in principle reduce the percolation threshold to about $x_c=0.061$,[15] thus shifting our ex-

TABLE II. Heights of the maximum in χ/x at T_a and T_b at 1000 Hz. If we would have fitted the microscopic time in Eq. (4b) as 10^{-9} sec instead of 10^{-11} sec, as suggested in Table I, we would have gotten 22.9, 22.6, and 12.9 for the theoretical maxima at T_b.

x	0.025	0.05	0.10
Theory T_a	183	57	11.0
Exper. T_a	67	29	9.4
Theory T_b	31.8	29.5	15.4
Exper. T_b	16.6	20.6	12.0

perimental concentrations $x = 0.025$, 0.050 closer to x_c, and producing therefore more and larger clusters at $T = 0$. Since we expect, however, that this interaction energy if it exists is small in comparison to $k_B T_b$, this effect is expected to be irrelevant for our purposes: only the spins strongly coupled at T_b should be included in our clusters.

The second effect, chemical clustering, could be more important and thus was investigated more quantitatively by performing a calculation where artificially the number of all triplets was doubled in the system to qualitatively simulate the effect that larger clusters occur with enhanced probability. The susceptibility curves then show additional anomalies, but of course do not cancel the maximum at T_b because these new anomalies still are much weaker than that of T_b. Thus chemical clustering would not affect drastically our conclusions.

Table II shows that the height of the maximum in the susceptibility per spin also agrees reasonably between theory and experiment. Again T_b is independent of the concentration and varies logarithmically in time, as is seen in the insert of Fig. 8. Thus, whereas T_a is independent of time, T_b decreases logarithmically in time, making clear that in this model the two characteristic times have different origins. Experimentally, the lower maximum also shifts somewhat with frequency, but the influence of the frequency on this maximum is smaller than on the other maximum at higher temperatures.

Thus the improved model accounts for most albeit not for all qualitative aspects of the experimentally observed susceptibility curves; and the complications did not destroy the good quantitative agreement with experiment found already from the simpler model in the temperature T_b.

VI. CONCLUSIONS

The present systematic experimental study of the ac magnetic susceptibility versus temperature in very dilute $(Eu_xSr_{1-x})S$ with $x = 0.025$, 0.05, and 0.10 has revealed two characteristic temperatures, T_a and T_b, both being dependent on frequency and concentration x, while in the static susceptibility no maximum has been observed in the range of accessible temperatures down to 7 mK. The double maximum in the curves of the ac susceptibility has been explained by a theoretical model of random clustering for the exchange-coupled Eu atoms, with dipole forces influencing the behavior of single clusters and the interaction of different clusters. The position T_b of the upper maximum was found to vary as $1/T_b \propto \log$ (time), independent on concentration for the samples with $x = 0.025$ and 0.05. Both features are in reasonable agreement between the experimental curves and the numerical calculations, without requiring free parameters or the knowledge of the exchange interaction constants. (We could identify that configuration of Eu atoms which produces the peak at T_b). The detailed shape of the observed anomaly depended on concentration x and frequency (time), which could be explained by our model.

Of course some discrepancies remain between experiment and present theory. In our dc experiments no anomaly is found around T_b, but still exists in our calculations at the corresponding time of 10^4 sec. Also no maximum is observed down to 7 mK in the static experiment whereas $T_a \approx 0.011$ K is predicted in the theory at $x = 0.05$. The experimental T_a depends much less on concentration and much more on frequency than the theoretical values. It seems that these discrepancies near T_a are due to our mean-field approximation of the dipolar cluster-cluster interaction.

From our experimental and theoretical studies on very dilute EuS we conclude that one may separate the forces being relevant for the blocking of the magnetization into three different classes according to their strength: (i) the strongest forces are the short-range exchange interactions which give rise to the Curie temperature T_c of 16.6 K for pure EuS. Thermal phenomena, where these exchange bonds are broken, are not discussed in the present paper but in earlier studies by Maletta *et al.*[23] These exchange interactions lead to clusters which are magnetically rigid at the low temperatures investigated here. (ii) Of intermediate strength are the dipole forces within one cluster; they produce energy barriers leading to blockage of clusters near $T_b \approx 0.2$ K. The Arrhenius law thus describes the frequency dependence. (iii) The weakest interactions are the fields exerted by the long-range dipole-dipole interaction between separated clusters, including isolated spins. In our model they lead to the other maximum near $T_a \approx 0.01$ K, which we believe is the most interesting result of our experiment and which needs further investigation.

ACKNOWLEDGMENTS

We thank Dr. H. Pink, Siemens AG, München, for preparation of samples, and Professor W. Zinn and Dr. K. Kehr for discussions. This work was part of the programs of SFB 65 and 125 and was supported financially by the Deutsche Forschungsgemeinschaft through SFB 65.

APPENDIX

This Appendix gives detailed cluster properties needed for the theoretical model and determines which of the many cluster configurations is responsi-

TABLE III. Cluster size s_k, perimeter t_k, magnetization m_k, multiplicity g_k, and energy barrier E_k (in Kelvin) for small clusters with s below 4. The index k corresponds to the numbers of Fig. 5.

k	s_k	t_k	m_k	g_k	E_k
1	1	18	1	1	0
2	2	26	2	6	1.55
3	2	30	0	3	0
4	3	31	3	8	2.34
5	3	34	3	12	0.54
6	3	34	3	24	1.86
7	3	34	3	6	3.29
8	3	37	1	24	1.47
9	3	38	1	24	1.24
10	3	41	1	12	0.36
11	3	42	1	3	0

ble for the anomaly at T_b.

For single spins, pairs, and triplets the magnetization m_k and energy E_k can be calculated easily. Single spins rotate freely without energy barriers. For pairs either the two magnetic moments are antiparallel to each other, directed perpendicular to the axis connecting their sites. Then the cluster magnetization and the energy barrier both are zero, and the pair is negligible. Or the two moments are parallel to each other, directed along the axis connecting their sites. Then the total magnetic moment of the cluster is nonzero, and because of its energy barrier the cluster contributes to long-time effects in the magnetization. Similar properties hold for the larger clusters. For the triplets the multiplicities g_k and perimeters t_k were counted by computer; the final results were found to be consistent with the series expansions of Ref. 15. Table III gives our result for the eleven cluster configurations depicted in Fig. 5.

The clusters with 4 spins each can be grouped into 62 classes $k=12$ to 73, with only the two extreme configurations shown in Fig. 5. The computer determined the perimeter, (varying between $t_{12}=36$ and $t_{73}=54$), the energy barrier (varying between 0 and 11 K), the magnetization (varying between 0 and 4, of course) but not the multiplicities g_k which were estimated by hand. (Comparison with Ref. 15 showed our g_k to be in the average about 10% too large, an error not important in our comparison with experiment and hardly relevant if we take into account the drastic approximations used for larger clusters as described below.) Inclusion of all four clusters shifted the susceptibility curves upwards but did not change the shape of the anomaly near T_b.

In order to be sure that this maximum is inherent

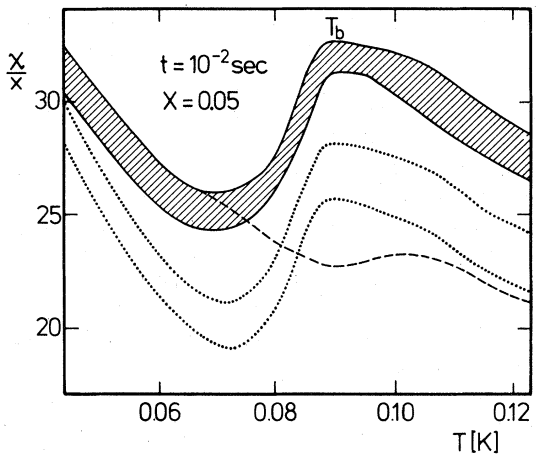

FIG. 9. Evidence that the maximum at T_b comes from configuration 2 of Fig. 5. The dashed line is calculated by omitting this configuration; the other lines take it into account. Data for $x=0.05$ at $t=10^{-2}$ sec.

in the model and not just due to the neglect of larger clusters we even estimated the influence of clusters up to size $s=10$ by the following approximations: A Monte Carlo simulation of the growth of random cluster configuration with size s produces many configurations from which the average perimeter $\langle t_s\rangle \equiv \sum_k t g_k / \sum_k g_k$ was estimated for every s. (In the sum only clusters with the same size s were employed, of course.) This perimeter was found to be 53, 61, 68, 76, 84, and 91 for $s=5,6,7,8,9$, and 10, respectively. Then for each size s, five different cluster configurations were selected and their energy E_k and magnetization m_k were calculated. These five examples were used in the sums of Eq. (7) to incorporate the large spread of energy barriers observed for each size s. The total number $\sum_k g_k(s)$ of configurations for a given size s (which according to our Table is 1, 9, and 113 for $s=1,2,3$) was estimated from Ref. 24 by the formula

$$\sum_k g_k(s) = A\lambda^s s^{-\tau}\exp(-Fs^{1-\theta})$$

with the "universal"[24] exponents $\tau=1.53$ and $\theta=1.65$, and with the lattice-dependent parameters $A=0.14$, $\lambda=13.94$, $F=0.65$ fitted on the data for $s=1,2$, and 3. This approximation gave 1645 for the total number of cluster multiplicities for $s=4$, whereas the exact result, as inferred from Ref. 15, is 1647.

As a further test of the accuracy of our cluster numbers for large clusters we calculated the ratio $\sum_k s_k n_k(x)/x$, summing up over those clusters we have taken into account with our approximations. If *all* clusters would be taken into account exactly, then this ratio would be unity (for x below the percolation threshold x_c) since[11,13] it represents the probability of an Eu atom to belong to any cluster of finite size.

(Note that we regard here single spins as clusters with size $s=1$). Our numerical result for this value on were 1.001 at 1%, 1.005 at 2.5%, and 1.000 at 5%, as desired. However, at 10% we found this ratio to be only 0.634 indicating that we cannot use our approximations that close to the critical concentration of 13.6%. Therefore we refrained here from quoting our results at that high concentration. But the exact result $n_1 = x(1-x)^{18} = 0.15\,x$ at $x = 0.10$. shows that for high concentrations the number of isolated spins and thus the height of the lower maximum at T_a is reduced, making the higher maximum near T_b appear more important.

We only sketched here the calculation of larger clusters since they are quite unimportant. They do not change the character of the anomalies; pairs and triplets are sufficient to give a nearly quantitative description of our model. This is shown in Fig. 9, based on Eq. (7). The upper curve, from Fig. 8, includes all clusters up to size 10. If any of the 8 triplet configurations is omitted, the resulting curve falls into the shadowed region of Fig. 8. If all clusters with $S_k \geq 5$ are omitted, we get the upper dotted curve; if all clusters with $S_k \geq 4$ are omitted one obtains the lower dotted curve. All these curves show still the pronounced maximum at $T_b = 0.1$ K. But if the ferromagnetically coupled pair, $K=2$, is omitted then we get the nearly monotonic dashed curve of Fig. 9. Thus this configuration, the nearest-neighbor pair, is mainly responsible for the maximum at T_b.

[1]For reviews see, e.g., V. Canella and J.A. Mydosh, AIP Conf. Proc. 18, 651 (1974); K. Binder, in *Festkörperprobleme* XVII, edited by J. Treusch (Vieweg, Braunschweig, 1977), p. 55.

[2]J.L. Tholence and R. Tournier, J. Phys. (Paris) 35, C4-229 (1974).

[3]F. Holtzberg, J.L. Tholence, and R. Tournier, in *Amorphous Magnetism* II, edited by R.A. Levy and R. Hasegawa (Pergamon, New York, 1977), p. 155.

[4]C.N. Guy, J. Phys. F 7, 1505 (1977).

[5]H. Maletta and W. Felsch, (unpublished).

[6]J.L. Tholence, F. Holtzberg, H. Godfrin, H.V. Löhneysen, and R. Tournier, J. Phys. (Paris) 39, C6-928 (1978).

[7]R. Frowein and J. Kötzler, Z. Phys. B 25, 279 (1976).

[8]Model 30 SQUID control, S.H.E. San Diego, Calif.

[9]G. Weber, Z. Phys. 171, 335 (1963).

[10]J.W.M. Livius and A.J. deVries, Appl. Sci. Res. 17, 31 (1966).

[11]D. Stauffer, Phys. Rev. Lett. 35, 394 (1975).

[12]L. Passell, O.W. Dietrich, and J. Als-Nielsen, Phys. Rev. B 14, 4897 (1976); see, however, W. Zinn, J. Magn. Magn. Mater. 3, 23 (1976), where a possible larger interaction range is discussed.

[13]J.W. Essam, in *Phase Transitions and Critical Phenomena*, edited by C. Domb and M.S. Green (Academic, London, 1972) Vol. II, p. 192.

[14]P.G. de Gennes, P. Lafore, and J. Millot, J. Phys. Chem. Solids. 11, 105 (1959).

[15]N.W. Dalton, C. Domb, and M.F. Sykes, Proc. Phys. Soc. London 83, 496 (1964).

[16]A. Messiah, *Quantum Mechnics* (North- Holland, Amsterdam 1968).

[17]More explicit calculations of relaxation rates due to higher-order dipolar processes can be found for some simpler cases in J. Kötzler, Physica (Utrecht) 60, 375 (1972); 60, 391 (1972).

[18]S.F. Edwards and P.W. Anderson, J. Phys. F 5, 965 (1975).

[19]K. Binder, Z. Phys. B 26, 339 (1977).

[20]A.J. Bray, M.A. Moore, and P. Reed, J. Phys. C 11, 1187 (1978); D. Stauffer and K. Binder, Z. Phys. B 30, 313 (1978).

[21]M.W. Klein, Phys. Rev. B 14, 5018 (1976), and references therein.

[22]K. Binder, J. Phys. (Paris) 39, C6-1527 (1978), and Ref.19.

[23]H. Maletta and W. Felsch, J. Phys. (Paris) 39, C6-931 (1978).

[24]A.J. Guttmann and D.S. Gaunt, J. Phys. A 11, 949 (1978).